Delft University of Technology

Moisture movement in cement-based repair systems monitored by X-ray absorption

Lukovic, Mladena; Ye, Guang; Schlangen, Erik; van Breugel, Klaas

Important note
To cite this publication, please use the final published version (if applicable).
Please check the document version above.

Moisture movement in cement-based repair systems monitored by X-ray absorption

M. Luković, Guang Ye, E. Schlangen, K. van Breugel
Delft University of Technology, the Netherlands

In concrete repair systems, material properties in the repair material and interface are greatly influenced by the initial moisture content of the concrete (or mortar) substrate. In order to quantify moisture profiles inside the repair system, X-ray absorption was used.

Preliminary studies are performed first to determine the absorption rate of a two-year-old mortar substrate. Cumulative water absorption and the penetration front of water are monitored as a function of time. Furthermore, absorption by the mortar substrate is investigated when a repair material is cast on top. Influence of water-to-cement ratio (w/c) of the repair material on water exchange, and moisture content change during drying in the repair system are studied. Ordinary Portland cement (OPC) paste was used as a repair material. It was shown that, initially, water from the repair material is absorbed by the substrate with the same speed as "free" water. Furthermore, not only can water be absorbed by the substrate, but it can also migrate back from the substrate to the repair material due to hydration of the repair material. Quantifying the dynamics of water exchange at an early stage between the repair material and the concrete substrate is a first step towards understanding the development of material and interface properties in repair systems. This can provide engineers with recommendations about substrate preconditioning in experiments and field practice.

Key words: X-ray absorption, water movement, repair system

1   Introduction

Moisture transport between cementitious repair material and concrete (or mortar) substrate determines the microstructural development of the interface and the repair material in concrete repair systems [Zhou 2010, Courard et al. 2011]. Capillary absorption by the concrete substrate is beneficial because it enables good mechanical interlocking

between the two materials [Courard 2000, Courard and Degeimbre 2003]. Apart from that, moisture absorption by the substrate prior to setting of the repair material also determines the resulting water-to-cement (w/c) ratio of the repair material. If too much water is absorbed by the substrate, there might not be enough water available for hydration of the repair material. Therefore, in order to obtain optimal performance of the repair system, the moisture exchange between repair material and substrate, and the repair system and the environment, should be well understood.

Still, this topic remains scarcely investigated and poorly explained, because the dynamics of water exchange is very complicated and strongly influenced by hydration of the repair material. As the microstructure of the repair material is continuously changing, the water diffusion coefficient of the repair material is dependent on time and initial water content of the concrete substrate. Only a few studies on moisture exchange in multilayer systems when fresh, newly cast material was placed on a matured substrate have been reported (Brocken et al. 1998, Faure et al. 2005, Kazemi-Kamyab et al. 2012). In all these studies, the nuclear magnetic resonance (NMR) technique was used. Some preliminary studies on layered "lego blocks" specimens made of freshly cast cement pastes were performed by using X-ray absorption (Bentz and Hansen 2000). Because both materials i.e., substrate and repair material, were freshly cast, these conditions did not directly imitate a repair system. In addition, most studies so far only indicated the relative change of moisture content by monitoring the change of the signal or measured spectra. Actual moisture content was only quantified in (Brocken et al. 1998).

In this paper, the possibility of using X-ray absorption technique for quantitatively studying moisture transport in a repair system was explored. First, the rate of moisture absorption of the mortar substrate was quantified. Sample preparation and a post-processing procedure for X-ray image data are explained. Furthermore, the absorption of the substrate when a fresh repair material is cast on top is investigated. OPC pastes with different w/c are used as repair materials. Samples were sealed for 3 days and during this period the moisture exchange was monitored. Subsequently, the repair materials in the repair system were exposed to drying from the top. Moisture profiles during drying are also quantified and critically evaluated.

2 Materials and methods

2.1 Materials and sample preparation

The substrate used in the study was a two-year-old mortar. A standard mortar mixture with OPC CEM I 42.5N, w/c of 0.5, cement-to-sand ratio 1 : 3 was used. Small prism specimens ($18 \times 19 \times 40$ mm^3) were cut with a diamond saw from bigger mortar samples. The mortar substrates were dried in an oven at 105 °C until constant weight was achieved. This was done in order to remove all evaporable water and create a zero initial moisture content at the beginning of the experiment (Hall 1989). It has to be noted that these conditions might trigger some microstructural changes and microcracking in the material (Ye 2003). The effects of thermal damage on capillary uptake of the cement paste were studied by Yang et al. (2014). It was shown that absorption rate of the thermally treated samples (preconditioned at 120 °C and 200 °C) is higher compared to those that underwent no thermal treatment. In current study it was important to have similar moisture conditions of all the substrate specimens prior to the application of the repair material. Therefore, possible microcracking of the substrates is considered not to affect the final conclusions.
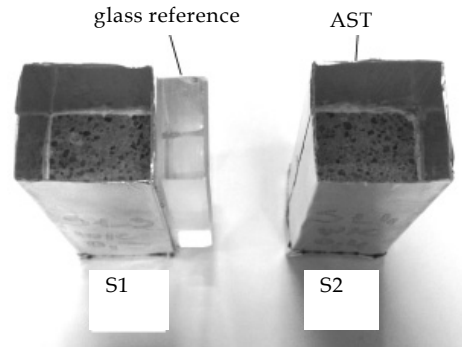
Prior to casting of the repair material, the top surface of the substrate was polished to minimize the influence of surface roughness (Fig. 1a). Two specimens (S1 and S2) with a sealant on the sides were then placed in a mould and covered with aluminium self-adhesive tape (AST) to prevent water evaporation from sides (Fig. 1b). A glass reference "specimen" was placed between the two samples in order to account for variations in beam intensity, as later explained. For repair materials, cement pastes with OPC CEM I 42.5 N and w/c of 0.3 and 0.4 were used. These pastes were cast on top of the mortar substrates and subsequently sealed.

### 2.2 X-ray absorption for moisture content measurements

After the preparation, two specimens were placed in a plastic container. Subsequently, container was placed in a Phoenix Nanotom X-ray system (Fig. 1c) where water exchange was measured. The apparatus is equipped for Computer Tomography (CT scanning), but in this study was limited to X-ray imaging without specimen rotation. A comparison between two X-ray images taken at the beginning and after a certain time step provides the moisture change in the sample at a certain time step. Temperature and relative humidity (RH) are not controlled in the X-ray system, however temperature and RH measuring devices (see in Fig. 1c) were placed in the chamber during testing.
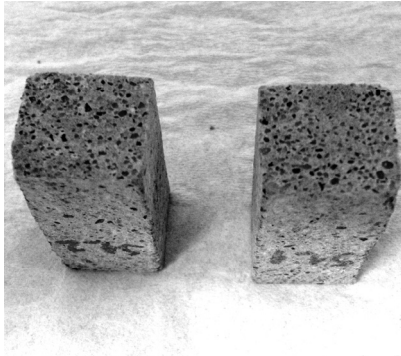
Mortar substrates after cutting and polishing   Substrates placed in moulds
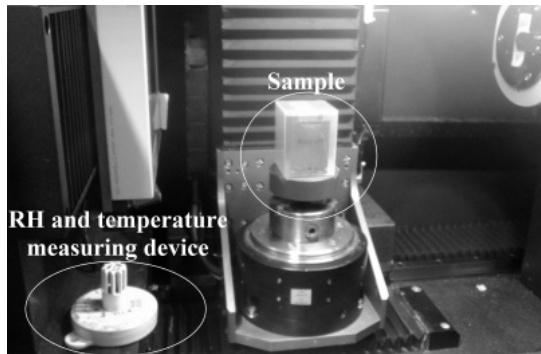
X-ray absorption setup with the position of the plastic container
(sample) and sensor for temperature and relative humidity (RH)

Figure 1: Preparation of the mortar substrate specimens and test set-up

When an object is irradiated with a bundle of X-rays, the X-rays are interacting with the material and are being attenuated (scattered and absorbed). The attenuation behaviour of monochromatic X-ray (X-ray photons of a single, consistent energy) can be described by the Beer-Lambert law (Michel et al. 2011):

$$I = I_0 \, e^{-\mu d} \tag{1}$$

where μ is the attenuation coefficient, d is the thickness of the sample and I_0 is the incident intensity. An attenuated X-ray results in transmitted intensity I. The detector visualises intensity levels as grey scale values (GSV) (Roels and Carmeliet 2006). Therefore, the attenuation coefficient of a material with a known thickness can be determined from the

change in intensity level, $\ln(I/I_0)$ (equation (1)), or, from the change in GSV, $\ln(GSV/GSV_0)$.

During moisture transport (either wetting or drying), the GSV of the material is changing. Correlating GSV change with the change in moisture content is done by making use of a simple physical principle. In a dry sample, X-rays are attenuated by the dry material only (Fig. 2-left). By scanning through the dry material, a reference image is obtained. If water is added to the porous material, the attenuating material will consist of the dry material plus a thickness of fictitious water layer, d_w, equivalent to the additional moisture content of the material (Fig. 2-right) (Roels and Carmeliet 2006). The additional moisture content is obtained by logarithmic subtracting a reference image from the image taken during moisture exchange. Therefore, provided that the change in beam intensity, $\ln(I/I_0)$, and attenuation coefficient of water are known, the (additional) moisture content inside the material can be determined according to equation (1). In this case I_0 corresponds to beam intensity after passing through the dry material while I corresponds to beam intensity after passing through the wet material. It has to be highlighted that this is a simplification.
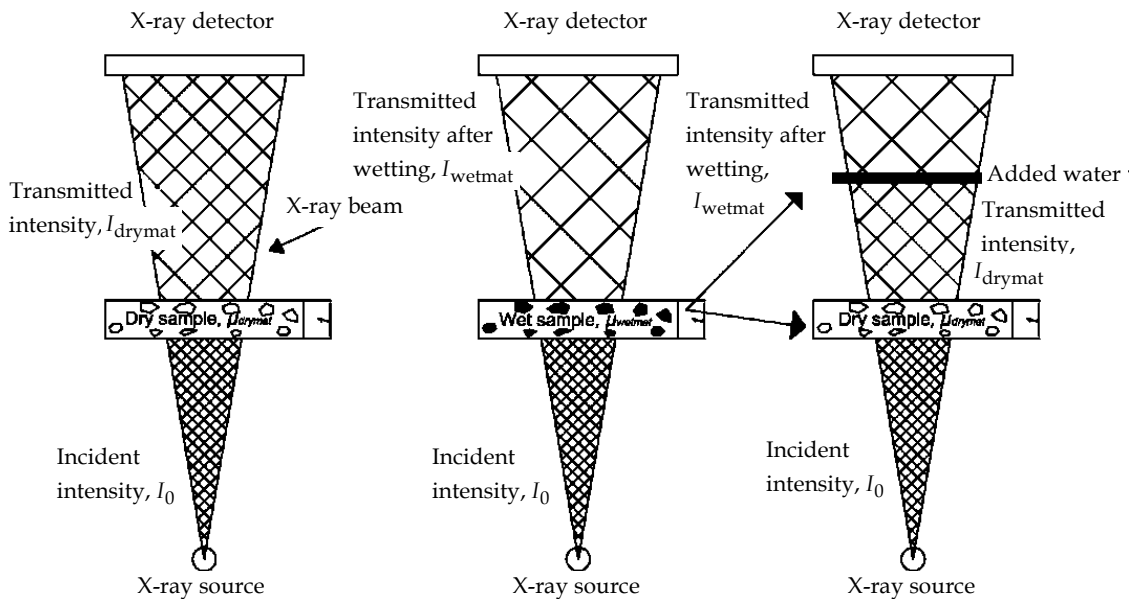

Figure 2: The moisture distribution is obtained by logarithmically subtracting an image of the dry sample I_{dry} from the image of the wet sample I_{wet}, adopted from (Roels and Carmeliet 2006)

Implications of this are further discussed in Section 2. 2. 1 when the attenuation coefficient of water is measured.

For quantification of the moisture content change, the following procedure was used:

- The attenuation coefficient of water can be determined based on the GSV change of empty and water filled containers with a known thickness (see Fig. 3a and 3b). The following formula is used:

$$GSV_{\text{water}} = GSV_{\text{air}}\, e^{\mu_{\text{water}} d_{\text{water}}} \tag{2}$$

- where GSV_{water} is the grey scale value of water, GSV_{air} the grey scale value of air, d_{water} is the thickness of the water layer (which is equal to the thickness of the container) and μ_{water} is the attenuation coefficient of water. The first image (Fig. 3a) is made with a beam passing through an empty container (and air surrounding the container) and GSV_{air} (corresponds to I_0) is obtained. The second image (Fig. 3b) is made with a container filled with water (beam is passing through container filled with water and air surrounding the container) and GSV_{water} (corresponds to I) is obtained. Thus, the unknown μ_{water} can be calculated based on equation (2) (derived from equation (1)).

- Once the attenuation coefficient of water is determined, GSV of the wet porous material can be correlated to GSV of the dry porous material according to the following equation (also derived from equation (1)):

$$GSV_{\text{water}} = GSV_{\text{drymat}}\, e^{-\mu_{\text{water}} d_{\text{w}}} \tag{3}$$

- where d_{w} is the thickness of fictitious water layer equivalent to the additional moisture content in the sample (see Fig. 2) and can be expressed as:

$$d_{\text{w}} = \Delta c_{\text{water}}\, \frac{d}{\rho_{\text{water}}} \tag{4}$$

- Here, Δc_{water} is the change of water content [g/cm³], d is the thickness of the sample and ρ_{water} is the density of water. From these equations, Δc_{water} can be determined as:

$$\Delta c_{\text{water}} = -\frac{\rho_{\text{water}}}{\mu_{\text{water}} d}\ln\frac{GSV_{\text{wetmat}}}{GSV_{\text{drymat}}} \tag{5}$$

- In order to exclude the influence of edges, only the middle part of the specimen (around 16 mm) is analysed (see Fig. 3c). The obtained moisture profiles are then averaged over the specimen's width. As a result, the change in moisture content is obtained as a function of specimen height. It is assumed that the water is distributed homogenously along the projection axes. In reality, however, the local moisture distribution might vary from the average.
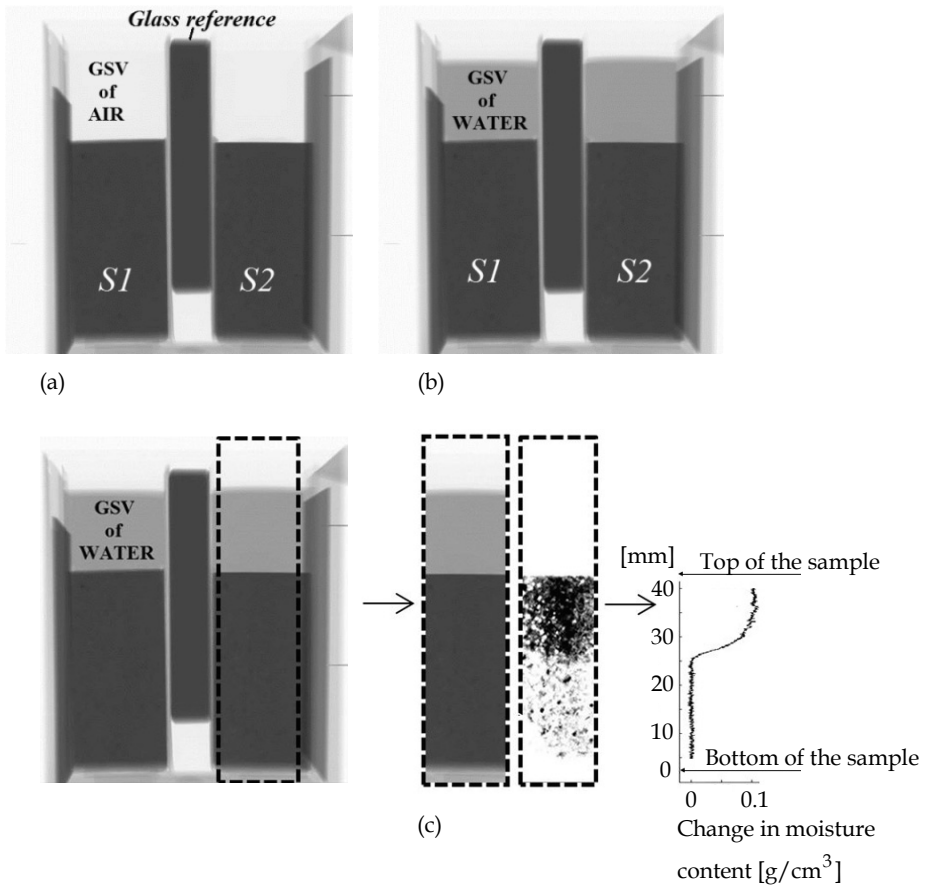

Figure 3: An example of the original X-ray images and analysis procedure: Difference in GSV between an empty (a) and water filled container (b) placed at the top of the specimens S1 and S2, used for calculating the attenuation coefficient of water (the objects left and right of the sample are the projections of the sample container), (c) analysed part of the specimen from which the moisture profile is calculated

Due to slight variations in the beam intensity, the obtained *GSV* varies even without a change in the moisture content. In order to account for this effect, a glass reference was used in all analyses (Fig. 3a). It is considered that glass does not absorb water and therefore, in this region, *GSV* should be constant during the measurement. Therefore, each image was normalised according to the variations of *GSV* of the glass reference in order to account for changes in the beam intensity.

The parameters for the X-ray imaging were set as: X-ray tube voltage 130 kV, X-ray tube current 270 µA. The spatial resolution was 30 µm/pixel. Each image used in the analysis (a representative image) is an average of 25 images. With 0.5 seconds needed for acquisition of an image, a representative image for a certain time step was obtained in 12.5 seconds.

2.2.1 Determination of the attenuation coefficient

When using polychromatic X-ray source (photons emitted over a range of energy levels), such as the one used in this research, two aspects should be considered in order to determine the attenuation coefficient of water (Pease et al. 2012).

The first aspect is that the attenuation coefficient of water depends on the water layer thickness. This dependency is a consequence of using polychromatic X-ray source, which leads to the so called "beam hardening" effect: while photons are passing through the material, lower energy X-ray photons are attenuated easier, the energy spectrum is changing, and progressively, with increasing thickness of material, remaining photons become "harder" to attenuate. As a result, the measured attenuation coefficient will depend on the thickness of the material. Attenuation provided by a certain thickness of a material is described by the term "effective attenuation coefficient". Pease et al. (2012) observed that, with the increasing thickness of the water layer (and also other materials such as clay brick, concrete and wood), the effective attenuation coefficient of material decreases. The effective attenuation coefficient of water in this research, measured for the different water layer thicknesses (Fig. 4), shows the same behaviour.

The second aspect is related to the beam hardening effect and the widely used principle of non-interacting composite system (Fig. 2), which assumes that the porous parent material does not influence the attenuation provided by water. In the absorption (or drying) tests, however, photons are attenuated both by the parent material and the water. Therefore, the attenuation coefficient of water cannot be determined independently of the parent material

28

(in this case mortar substrate). In order to account for this, Pease et al. (2012) introduced the term "coupled effective attenuation coefficient" of water, which is a function of the parent material and its thickness. They observed that, with increasing thickness of different materials (e.g. concrete, cement paste, calcium silicate, etc.), the coupled effective attenuation coefficient of water decreases. In this research, the same was tested by placing the 18 mm thick mortar substrate in front of the water holder (with inner dimensions of 4 mm, 9 mm and 33 mm). The obtained coupled effective attenuation coefficient of water was lower than the effective one (Fig. 4), similar to the findings of Pease et al. (2012).
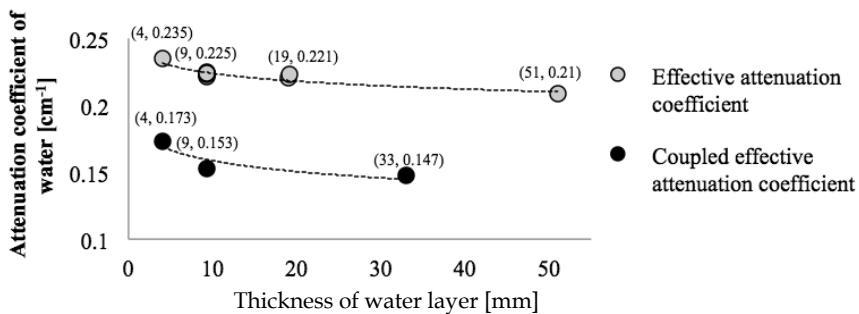

Figure 4: Influence of water layer thickness and parent material (mortar substrate) on measured attenuation coefficient of water

The thickness of the water layer used for determining the attenuation coefficient of water should, therefore, correspond to the anticipated maximum change of the water content in the parent material. In this case the attenuation coefficient of the 4 mm thick water layer , placed behind the 18 mm thick mortar substrate, measured to be 0.1728 cm^{-1}, was used further to quantify the change of the water content. Accordingly, the maximum change of the water content in the mortar substrate is assumed to be around 0.22 g/cm^3, which is reasonably close to the maximum moisture content of the mortar.

2.2.2 Limitations of the experiment

An important limitation of the technique is caused by the conical beam of the X-ray setup. As a result, the thickness of the material through which the beam passes depends on the position of the source with respect to the specific location (i.e. coordinate) in the sample (Fig. 5a). Consequently, at the top and the bottom of the sample, the thickness of the attenuating material is larger, and this will affect the effective attenuation coefficient. The thickness of the sample through which the beam is passing varies between 18 mm in the

middle of the specimen (i.e. when the beam is perpendicular to the specimen) to 18.16 mm at the top and bottom (Fig. 5a). In the current research, this was not taken into account, but should be considered for improvement of the technique.

One more consequence of the conical beam is that X-ray photons are not emitted parallel to the repair/substrate interface. The interface location, therefore, is not well defined, and it includes a small zone of both the repair material and the substrate. The scattering process of the X-ray beam is, therefore, modified in this zone. The width of this zone was estimated
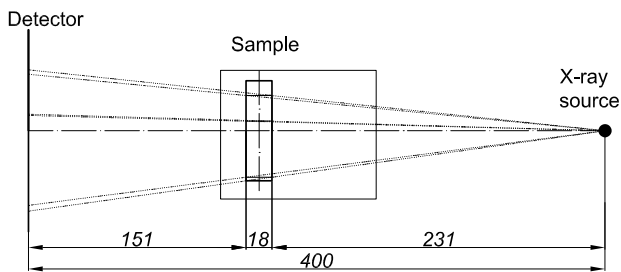
Position of the detector, the specimen and the source
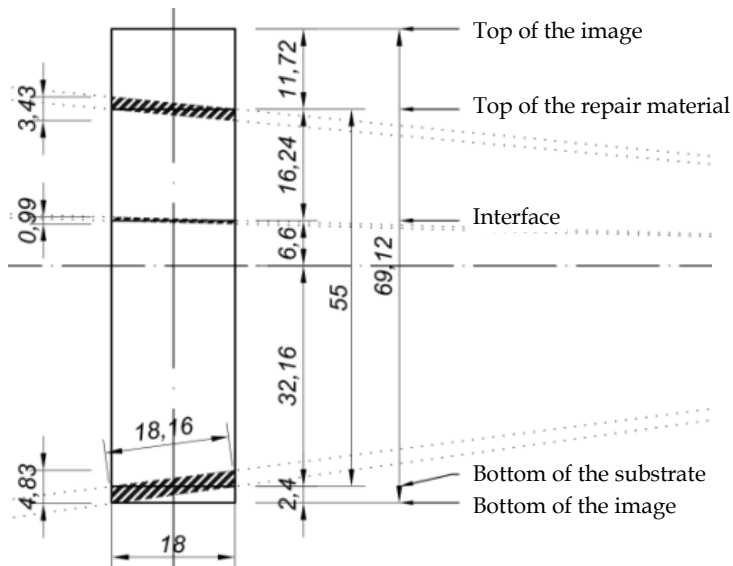
Beams passing through the sample, high magnification

Figure 5: Experimental setup and influence of the conical beam on the measured data, lengths are in [mm]

to be around 1 mm (Fig. 5b). This interfacial zone is marked further in the article with the dashed line (with a thickness of around 1 mm) to indicate the unreliability of the results in this zone. Similarly, the bottom and the top of the specimen are also affected (4.83 mm and 3.43 mm, respectively, see Fig. 5b), and these parts were excluded from the graphs. Note that these effects are dependent on the specimen thickness and the distance between the object and the source.

2.3 *Gravimetric test*

Gravimetric tests were performed in order to verify results obtained by X-ray absorption. Same samples with the same preparation procedure as for X-ray testing were used. The gravimetric test was performed according to the standard for determination of capillary absorption in concrete and mortar (NEN-EN 480-5, 2005).

3 Absorption by the mortar substrate

The first study deals with the absorption rate of the mortar which was used as a substrate. Substrates were always placed vertically in the set-up but water absorption was investigated both when water was absorbed from the bottom and from the top of the substrate. This was done in order to investigate the influence of gravity, as the repair material would be cast at the top of the substrate.

3.1 *Absorption by the mortar substrate when water is absorbed from the bottom*

Two replicate specimens were tested (marked as ABS-bottom-S1 and ABS-bottom-S2). A reference image was made before exposing substrates to water absorption. X-ray images (Fig. 6) indicate moisture change as a function of time. As material is absorbing more water with time, the moisture front is moving up and GSV of material is changing.
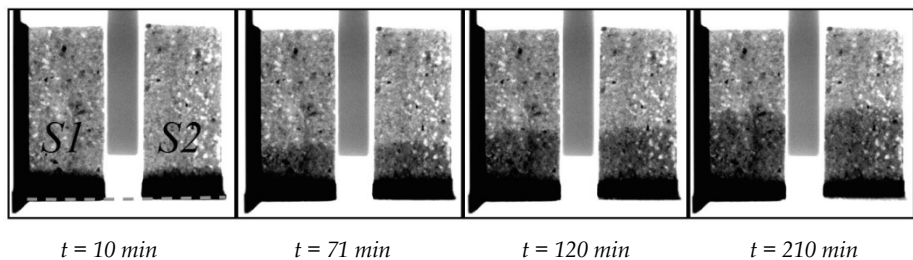

| t = 10 min | t = 71 min | t = 120 min | t = 210 min |

Figure 6: Qualitative representation of the substrate absorption as a function of time;
wetting from the bottom, test marked as ABS-bottom

Quantitative moisture profiles as a function of time (uptake in vertical direction) are given in Fig. 7. In order to exclude air, graphs do not start from the bottom of the image, but from the bottom of the samples (dashed line in Fig. 6). Measurements in the bottom part of the mortar (which gets immediately in contact with water) are unreliable (Fig. 5b) and are excluded. As previously explained, the moisture profile is averaged over the specimen width (16 mm) and specimen thickness (18 mm). Moisture profiles are very uniform, indicating that the sample is quite homogenous (at mm scale). 2D moisture fronts given in Fig. 6 (average only over specimen thickness) also confirm this uniformity. Based on measurements by this technique (X-ray micro computed tomography) and for the resolution of 30 µm, no microcracking is observed in the mortar (Lukovic and Ye 2016, Lukovic 2016). Obtained curves resemble in shape to those obtained by neutron radiography (Zhang et al. 2010) or nuclear magnetic resonance method (Hall 1989).
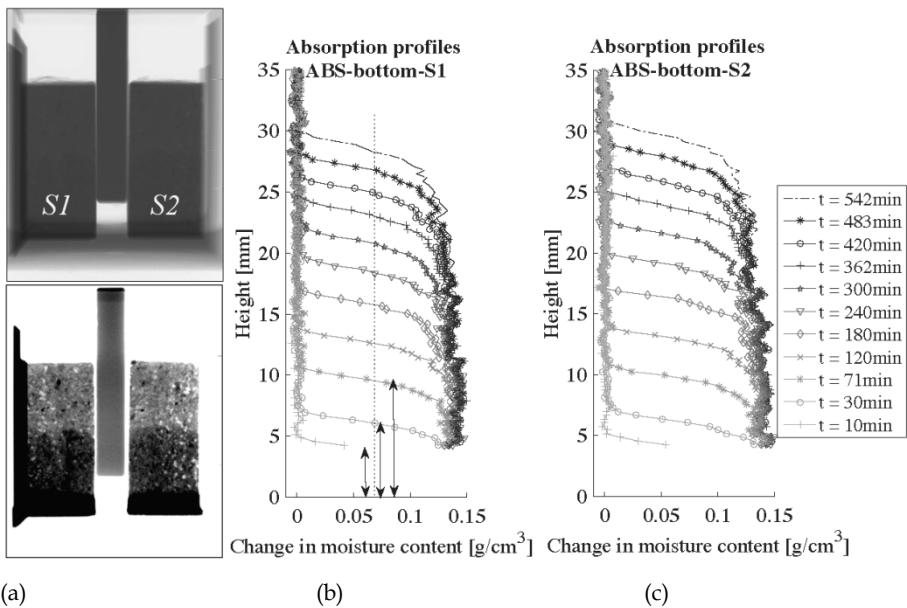

(a)　　　　　　　　　　　　　(b)　　　　　　　　　　　　　(c)

Figure 7: Moisture profiles in specimens as a function of time (ABS-bottom): (a) Obtained image, t=240 min (top – whole GSV range and bottom – chosen GSV range), (b) Moisture profiles in ABS-bottom-S1 as a function of time, (c) Moisture profiles in ABS-bottom-S2 as a function of time, moisture profile represents the averaged water content of the material at certain point in time over the specimen height

3.2   Absorption of the mortar substrate when water is absorbed from the top

Additionally, absorption of the substrate with a water layer on top is investigated. Results are presented in Fig. 8. Two replicate specimens were tested (ABS-top-S1 and ABS-top-S2). Obtained moisture profiles are similar to those obtained in the previous section (Fig. 7b and 7c).

3.3   Comparison of the results and discussion

In order to compare the rate of absorption in two cases, inflection points are defined (chosen at 0.07 g/cm³) and the absorption rate is calculated. The first three inflection points are indicated in Figs. 7b and 8b. Absolute differences between the inflection points at certain time steps and the specimen bottom (indicated by arrows in Figs. 7b and 8b) are defined as absorption profile (height). The absorption profile, which is a linear function of square root of time within the monitored time, is given in Fig. 9. It can be observed that the absorption direction (i.e. gravity) does not have a significant influence on water absorption. A similar effect was observed by (Hall and Hoff 2007) when studying the
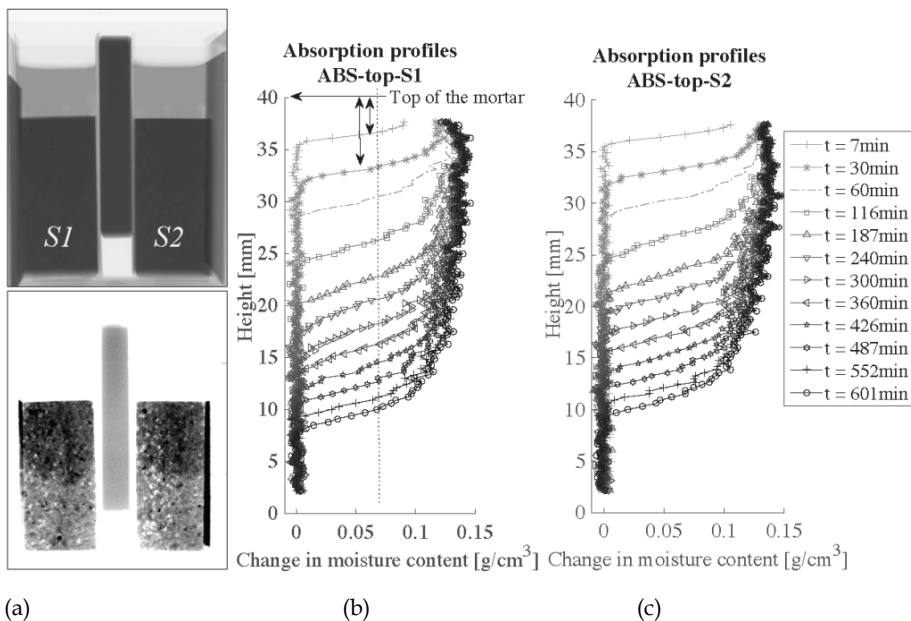

(a)   (b)   (c)

Figure 8: X-ray absorption results when water is absorbed from the top (test marked as ABS-top): (a) Obtained image, t=240min, (top – whole GSV range and bottom – chosen GSV range), (b) Moisture profiles in ABS-top-S1 as a function of time, (c) Moisture profiles in ABS-top-S2 as a function of time
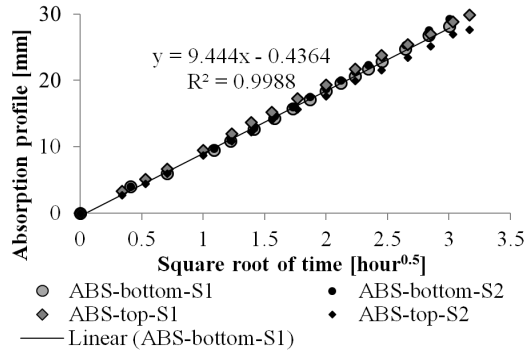
Figure 9: *Absorption profiles in the specimens where water was absorbed from the bottom and from the top*

capillary rise dynamics in walls. They concluded that, due to dominance of capillary forces, gravity, in most cases, can be neglected.

Gravimetric tests were performed to verify the results obtained by X-ray absorption. With a gravimetric test, only the total amount of water absorbed as a function of time can be measured. To compare the results, the total amount of absorbed water measured by X-ray absorption is calculated by integrating the moisture profile at a certain time step. Results are given in Figure 10.
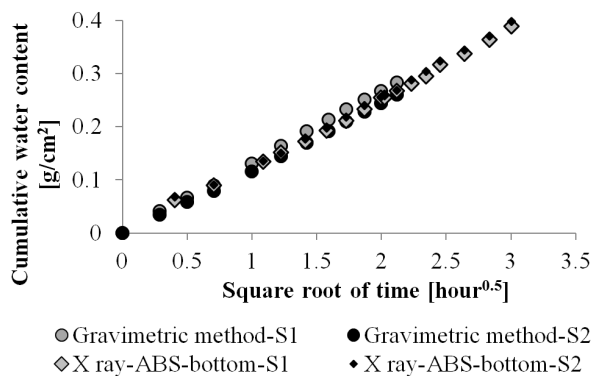

Figure 10: *Comparison between moisture absorption measured by gravimetric test and by X-ray absorption*

Both tests show that the capillary absorption follows a linear function of square root of time within the monitored time (Figs. 9 and 10). Based on this coefficient of capillary suction (slope in Fig. 10), an effective radius representing the pore size distribution of the mortar can be calculated (Zhang et al. 2011). In addition, Boltzmann transformation can be applied to the measured profiles and moisture diffusivity can be obtained (Lukovic et al. 2015). Moisture content measured by X-ray absorption is very close to the results obtained with the gravimetric test. This means that the measured coupled effective attenuation coefficient of water is in a reasonable range and can be used further for the quantification of the water content.

Moisture profiles obtained by X-ray absorption are similar to the results obtained by other techniques for the same type of material. Most of the other techniques for monitoring moisture movement are one - dimensional, meaning that only one point is scanned at a time (Roels and Carmeliet 2006). An advantage of X-ray absorption is that it is very fast and, similar to neutron radiography, it provides 2D moisture content maps. Therefore, with X-ray, moisture exchange can be monitored with very high spatial (in this case 30 µm) and temporal (images can be made every 0.5 s) resolution. For this study, though, even lower spatial and temporal resolution would have probably been sufficient. A disadvantage is, however, that a conical X-beam is used, which affects the scattering process (Fig. 5b). In addition, the obtained moisture profiles (2D images) are averaged over the scanning thickness, meaning that only the bulk response is obtained. By applying computed tomography an extension of the method to 3D could be made (Roels and Carmeliet 2006), but then the temporal resolution would be reduced. Another disadvantage of standard X-ray absorption versus neutron radiography and NMR is that the effects of hydration (a portion of water is becoming chemically bound) cannot be captured. This is because the total mass of water in the repair material specimen (and therefore, the bulk density of the repair material) is not changing during hydration. As explained by Prade et al. (2015), the attenuation of X-rays is dominated by photoelectric absorption and varies with the atomic number of the element. Since during hydration, the atomic number of elemental constituents in the cement paste is not changing, the attenuation coefficient remains constant during reaction. Therefore, only the water movement, but not the hydration are detected. Yang et al. (2014) and Prade et al. (2015) studied moisture transport and cement hydration by recently developed X-ray dark-field imaging. This technique enables to analyse microstructural development and setting

processes during hydration within macroscopic samples, at sub-pixel resolution. In future, advances and combinations of different approaches for X-ray imaging can be used to provide valuable information on materials and systems with both on-going hydration and moisture movement (i.e. cement based repair systems).

4   Moisture movement in the repair system

4.1   Moisture movement in the repair system during sealed curing

Cement pastes with a w/c of 0.3 and 0.4, and around 15 mm thickness were cast on the top of the dry substrate mortar which was previously dried at 105 °C. The two systems are marked as w/c = 0.3, DS, S2 and w/c = 0.4, DS, S2 respectively. Immediately after casting, the repair systems are sealed with aluminium self-adhesive tape and placed in the X-ray system in order to investigate the moisture exchange between repair material and mortar substrate (Fig. 11). The tests lasted 5 days and the average temperature and relative humidity during the experiment were 26 °C and 24% with standard deviations of 1 °C and 4%, respectively.
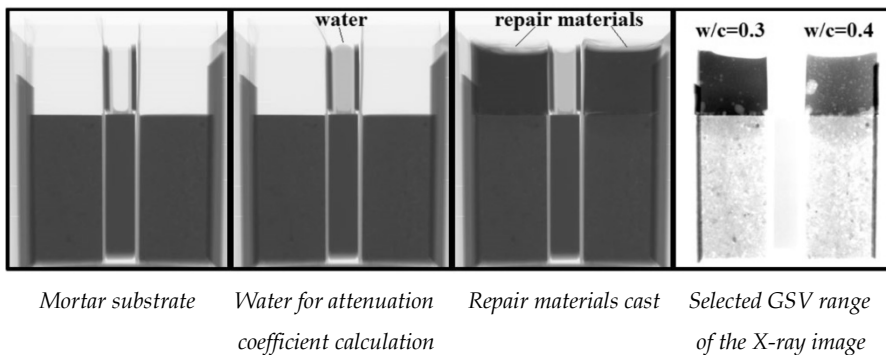

| Mortar substrate | Water for attenuation coefficient calculation | Repair materials cast | Selected GSV range of the X-ray image |

Figure 11: X-ray measurements on repair systems inside the X-ray chamber
(w/c = 0.3, DS, S2 and w/c = 0.4, DS, S2)

It is assumed that the main substance absorbed by the mortar substrate from the repair material is water. Therefore, although cement slurry (and not pure water) is probably absorbed by the mortar substrate, the coupled effective attenuation coefficient of water is used in the calculations.

The reference image was made 30 minutes after mixing the repair material, which was the time needed for casting, vibrating, sealing and placing the specimens in the X-ray system. The first measured profile is obtained 2 minutes after making the reference image and 32 minutes after mixing the repair material (Fig. 12). As a consequence, the change in moisture profiles at the top of the substrate (close to the interface) could not be captured. These parts (indicated by a dashed rectangle in Fig. 12a and 12b) are filled with water during the initial 30 minutes. As previously discussed, the interface is not parallel to the X-
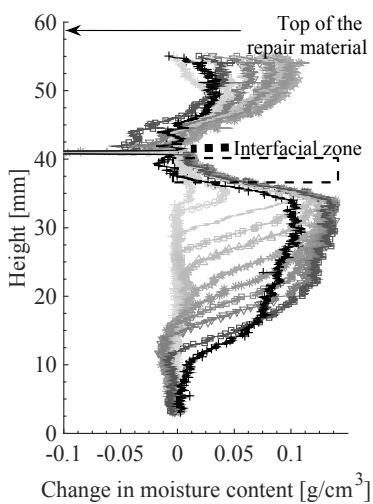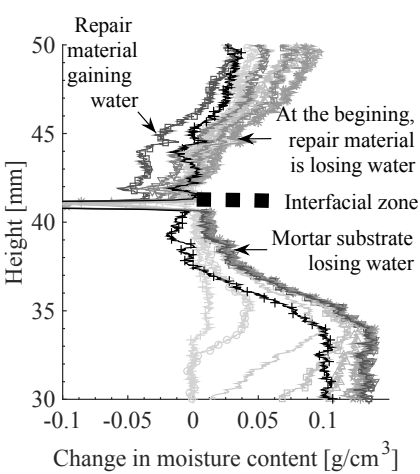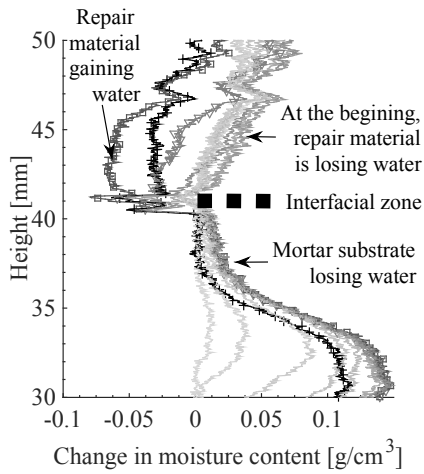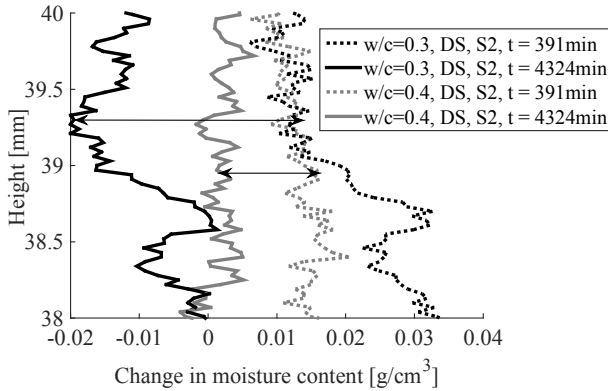

(a) *w/c = 0.3, DS, S2*
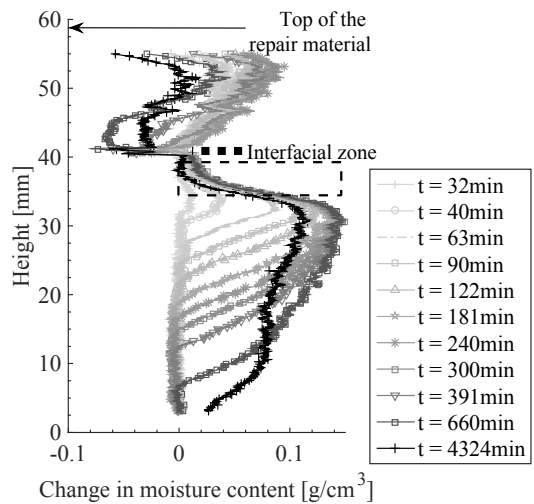
(b) *w/c=0.4, DS, S2*

(c) *Legend*

(d) *magnified profiles close to the interface*
w/c = 0.3, DS, S2

(e) *magnified profiles close to the interface*
w/c = 0.4, DS, S2

(f) *Water loss from the substrate close to the interface in w/c = 0.3, DS, S2 and w/c = 0.4, DS, S2*

Figure 12: Moisture profiles in the repair systems as a function of time, t
(time refers to time after mixing the repair material)

ray beam and, therefore, the multiple scattering process is modified in this zone. Therefore, the results in this zone are not reliable and are indicated by the dashed line.

The total amount of absorbed water in the substrate as a function of time (starting from 32 minutes) was calculated by integrating moisture profiles in the substrate at each time step (Fig. 13). In the first 5 hours, both mortar substrates absorbed the same amount of water. In addition, these curves have a similar slope as the curves obtained in the absorption test (previously given in Figs. 7 and 8). Therefore, the cement slurry from the repair material is absorbed with the same rate as "free" water in the first 5 hours (Fig. 13). In addition, the absorption rate by the substrate does not depend on w/c of the repair material. Similar observation is made for the speed of absorption of water by the brick in a mortar-brick composite (Caspar, Larbi, 1999). As water from the repair material can be absorbed very fast, hydration of the repair material might be hindered because a lower amount of water (compared to designed) stays in the repair material. It seems, therefore, that pre-saturating the mortar (or concrete) substrate is a critical factor for obtaining expected repair system properties.

Although the initial absorption rate is similar, the final amount of water that is absorbed in the two systems (w/c = 0.3, DS, S2 and w/c = 0.4, DS, S2) is different. This is caused by the different w/c of the two repair materials. The repair material with w/c = 0.3 exhibits faster reduction in the rate of absorption than the material with w/c = 0.4. Furthermore, water
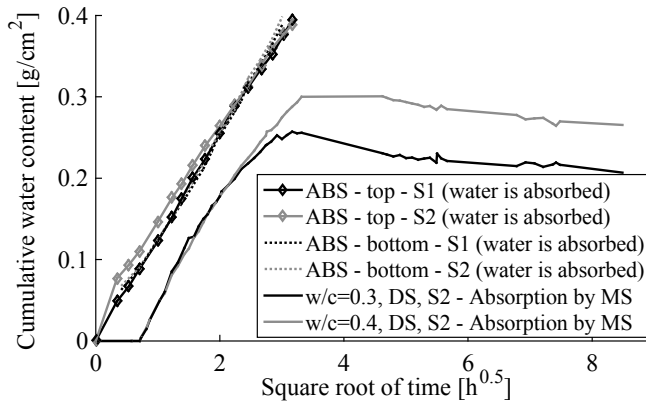
Figure 13: Cumulative moisture absorption of the mortar substrate (MS) from repair material w/c=0.3, DS, S2 and w/c=0.4, DS, S2 compared to cumulative moisture absorption when water is absorbed

from the substrate migrates back to the repair material. That can be seen from the negative shift in the substrate (indicating moisture loss) in moisture profiles (Figs. 12d and 12e). At the bottom of the repair material (5 - 7 mm to the interface), after 660 minutes, moisture profiles have a positive shift indicating water gain. In the repair material, there are two causes of water loss: water taken by the unsaturated substrate and hydration reaction of the material itself. Hydration of the repair material causes the consumption of capillary water from the repair material, thereby reducing the relative humidity that, at a certain point in time, was in equilibrium with the substrate. Therefore, a new capillary pressure potential difference is created. In order to restore the equilibrium state, water is driven back from the substrate to the repair material. In the material with the lower w/c (0.3), there is a higher pressure difference due to the finer pores and lower amount of available water. As a result, more water will flow back from the substrate. As a result, the shift in substrate profiles close to the interface is twice as large in the repair system with w/c = 0.3 compared to the system with w/c = 0.4 (Fig. 12f).

In order to perform the integration procedure and calculate the cumulative water content for the whole repair system, three integration limits are defined: top of repair material (top arrow in Figures 12a and 12b, defined as the repair material height immediately after casting), interface (dashed line) and bottom of mortar substrate (where the moisture profiles begin). In these calculations it is assumed that the coupled effective attenuation coefficient of the water in the repair material is equal to the coupled effective attenuation

coefficient of the water in the mortar substrate. In Figure 4 it was shown, however, that the coupled effective attenuation coefficient is sensitive to the porous material thickness and the thickness of the water layer. These are not the same for the repair material with w/c of 0.3 and 0.4 (i.e. 23% and 29% of water by mass of paste respectively) and the mortar substrate with w/c of 0.5 (i.e. 66% of aggregates and 11% of water by mass of mortar). Furthermore, the calculation of the water movement within the repair material is very complex because of the on-going hydration and the volume changes in the material. The height of the repair material is changing (due to setting in the early stage and later due to shrinkage). In addition, due to the conical beam effects, the interface location cannot be precisely defined. Having in mind all these assumptions and simplifications, further calculations for the water content inside the repair material should be taken only as indicative.

The cumulative water content as a function of time is then calculated for the repair material, the substrate and the whole repair system. Curves are given in Figure 14a. The substrate is absorbing water (cumulative water content is positive), while the repair material is losing water (cumulative water content is negative). If the calculation procedure and sealing are perfect, the cumulative water content in the system should be equal to 0 (i.e. the amount of water that is lost from the repair material should be equal to the amount of water that is absorbed by the substrate). As both aluminium foil and sealant are used for sealing of specimens, it is considered that the sealing procedure is good, but that numerous assumptions in the calculation (as previously explained), led to differences in calculated cumulative water contents in the system.

4.2 *Moisture exchange in the repair system during drying*

In the first 72 hours of curing, samples were sealed and the water content in the repair system is constant (Fig. 14a). After 72 hours from casting, the repair systems were exposed to drying. Reference image for drying profiles is the image taken immediately after uncovering the samples. The moisture content in the repair systems starts decreasing due to drying. More water is lost from the system with a higher initial w/c (Fig. 14b).

Moisture profiles of the two drying specimens are shown in Figs. 15a and 15b and they confirm that moisture profiles during drying can also be accurately captured with X-ray absorption. After 7 hours of drying, there is no significant difference between the two moisture profiles. However, after 45 hours more water is lost from w/c = 0.4, DS, S2

compared to w/c = 0.3, DS, S2. Note that in both specimens, at later drying times, the substrate starts losing water, but there is no water loss from the repair material close to the interface. This might indicate that big pores in this region do not contain water. Water is probably only present in the hydration products (gel) and in fine pores, and therefore, is
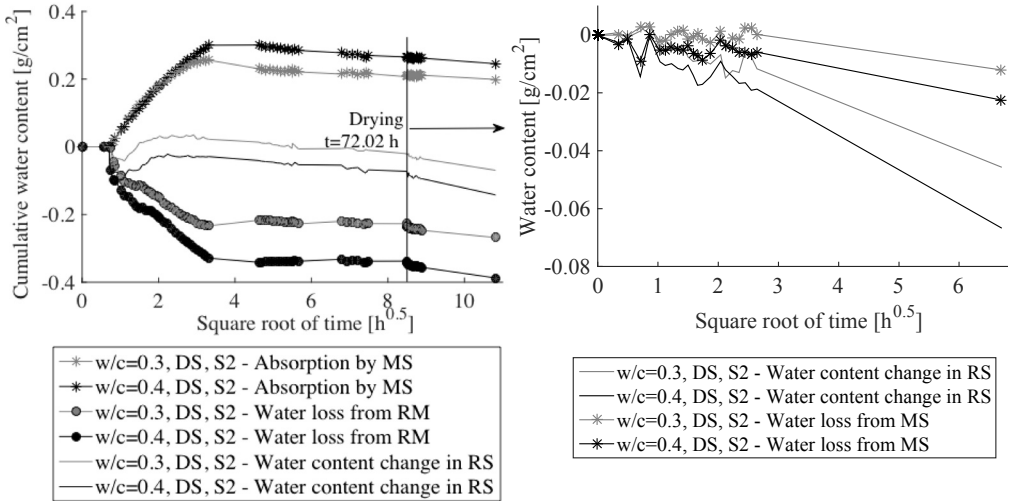
(a) *Cumulative water content in the repair system*   (b) *Water loss from the onset of drying*

Figure 14: Cumulative water content in the repair systems w/c = 0.3, DS, S2 and w/c = 0.4, DS, S2
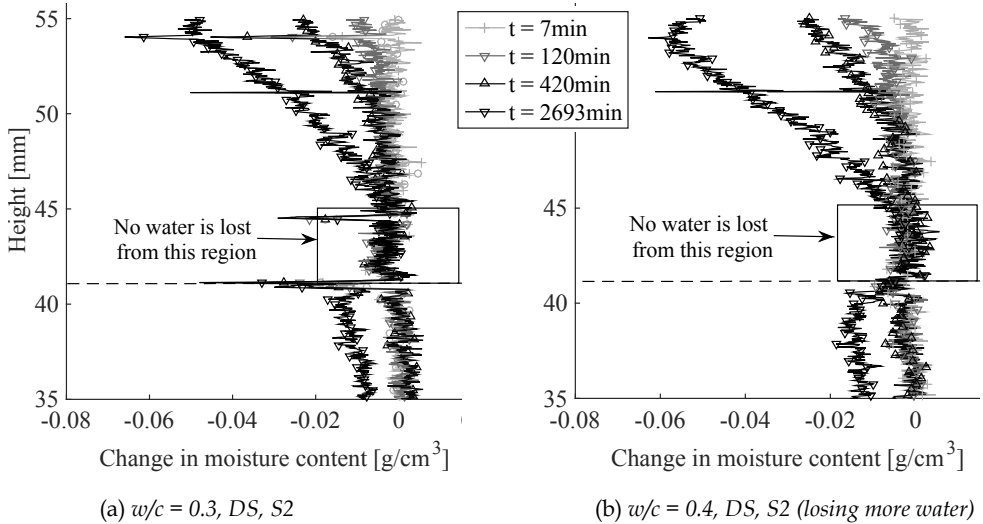
(a) *w/c = 0.3, DS, S2*   (b) *w/c = 0.4, DS, S2 (losing more water)*

Figure 15: Drying profiles in repair systems

not available for evaporation under these drying conditions. An initially dry substrate (dry prior to application of repair material) leads to lack of water in the repair material in the region close to the interface. Although some water is taken back from the substrate (Fig. 12), deficiency of water can have negative influence on hydration rate of the material and cause lower strength in this region. In addition, in previous research it was found that a higher substrate absorption leads to a significantly higher void content close to the interface in the repair system (Lukovic, Ye, 2016). A higher void content may further decrease the material strength in this region.

5   Conclusions

In this paper, X-ray absorption is used to accurately monitor moisture movement in porous materials with a high spatial and temporal resolution. Changes in moisture content both during absorption and drying are monitored and quantified. With this technique, the dynamics of moisture exchange in repair systems are investigated. Based on the presented study and the investigated parameters, the following conclusions are drawn:

- Water absorption as a linear function of the square root of time within the monitored time (during the initial 9 hours) can be observed.
- In the first 5 hours after casting, the w/c of the repair material is not affecting water loss from the repair material. Furthermore, water from the repair material is absorbed by the substrate with the same rate as pure, "free" water. Water lost due to the absorption by the substrate reduces the initial amount of water in the repair material. Water exchange in a repair system, therefore, has a critical influence on the microstructure formation of the bulk repair material and the interface.
- At later age, water movement back from the substrate to the repair material was observed. The lower the w/c of the repair material, the higher the movement is.
- The drying rate of repair material is higher when the repair material has a higher w/c. From the moisture profiles during drying, it can be inferred that the biggest pores in the region close to the interface in the repair material, cast on an initially dry substrate, are probably empty.

It should be emphasised that, in order to reduce heterogeneity, a model material (cement paste instead of mortar or concrete) was used as a repair material. For practical

42

applications, paste will never be used. A bigger particle size in the repair material affects the size of the interface between the repair material and mortar substrate. Therefore, when mortar and concrete are used as repair materials, conclusions from this paper need to be applied with caution. Furthermore, more realistic drying conditions, without thermal treatment of the substrate should be applied in future.

The X-ray technique presented here can be improved and the same samples should be also tested by different methods (i.e. neutron radiography, NMR) to compare the results. In addition, a sensitivity study of the coupled effective attenuation coefficient for cement paste and mortar with different w/c and aggregate content should be performed in order to improve the X-ray measurement procedure.

Literature

Bentz D, Hansen K (2000) Preliminary observations of water movement in cement pastes during curing using X-ray absorption. *Cement Concrete Res* 30(7): 1157-1168

Brocken H, Spiekman M, Pel L, Kopinga K, Larbi J (1998) Water extraction out of mortar during brick laying: a NMR study. *Mater Struct* 31(1): 49-57

Courard L (2000) Parametric study for the creating of the interface between concrete and repair products. *Mater Struct* 33(1): 65-72

Courard L, Degeimbre R (2003) A capillary action test for the investigation of adhesion in repair technology. *Can J Civil Eng* 30(6): 1101-1110

Courard L, Lenaers JF, Michel F, Garbacz A (2011) Saturation level of the superficial zone of concrete and adhesion of repair systems. *Constr Buil Mater* 25(5): 2488-2494

Faure P, Caré S, Po C, Rodts S (2005) An MRI-SPI and NMR relaxation study of drying–hydration coupling effect on microstructure of cement-based materials at early age. *Magn Reson Imaging* 23(2): 311-314

Groot CJWP, Larbi J (1999) The influence of water flow (reversal) on bond strength development in young masonry. *HERON*, Vol. 44 (2).

Hall C (1989) Water sorptivity of mortars and concretes: a review. *Mag Concrete Res* 41(147): 51-61

Hall C, Hoff WD (2007) Rising damp: capillary rise dynamics in walls. *P R Soc Lond A Mat* 463(2084): 1871-1884

Kazemi-Kamyab H, Denarie E, Bruhwiler E, Wang B, Thiery M, Faure PF, Baroghel-Bouny V (2012) Characterization of moisture transfer in UHPFRC-concrete composite systems at early age. Proceedings of Second International Conference on Microstructural-related Durability of Cementitious Composites. Amsterdam, the Netherlands

Lukovic M, Ye G, Schlangen E, van Breugel K (2015) Monitoring and modelling of capillary moisture uptake in mortar, Proceedings of the 14th International Congress on the Chemistry of Cement (ICCC 2015)

Lukovic M, Ye G. (2015) Effect of Moisture Exchange on Interface Formation in the Repair System Studied by X-ray Absorption. *Materials*, 9(1), 2.

Lukovic M (2016) *Influence of interface and strain hardening cementitious composite (SHCC) properties on the performance of concrete repairs*. Dissertation, Delft University of Technology

Michel A, Pease BJ, Geiker MR, Stang H, Olesen JF (2011) Monitoring reinforcement corrosion and corrosion-induced cracking using non-destructive x-ray attenuation measurements. *Cement Concrete Res* 41(11): 1085-1094

NEN-EN 480-5 (2005) Admixtures for concrete, mortar and grout-test methods-part 5: Determination of capillary absorption

Pease BJ, Scheffler GA, Janssen H (2012) Monitoring moisture movements in building materials using X-ray attenuation: Influence of beam-hardening of polychromatic X-ray photon beams. *Constr Buil Mater* 36: 419-429.

Prade F, Chabior M, Malm F, Grosse CU, Pfeiffer F (2015) Observing the setting and hardening of cementitious materials by X-ray dark-field radiography. *Cement Concrete Res* 74 (2015): 19–25

Roels S, Carmeliet J (2006) Analysis of moisture flow in porous materials using microfocus X-ray radiography. *Int J Heat Mass Tran* 49(25): 4762-4772

Yang F, Prade F, Griffa M, Jerjen I, Di Bella C, Herzen J, Sarapata A, Pfeiffer F, Lura P (2014) Dark-field X-ray imaging of unsaturated water transport in porous materials. *Appl Phys Lett*, 105(15).

Ye G (2003) *Experimental study and numerical simulation of the development of the microstructure and permeability of cementitious materials*. Dissertation, Delft University of Technology

Zhang P, Wittmann F. H, Zhao T, Lehmann E, Jin Z (2010) Visualization and quantification of water movement in porous cement-based materials by real time thermal neutron radiography: Theoretical analysis and experimental study. *Science China Technological Sciences* 53(5): 1198-1207

Zhang P, Wittmann F. H, Zhao T. J, Lehmann E. H, Vontobel P (2011) Neutron radiography, a powerful method to determine time-dependent moisture distributions in concrete, *Nucl Eng Des* 241(12): 4758-4766

Zhou J (2010) *Performance of engineered cementitious composites for concrete repairs*, Dissertation, Delft University of Technology